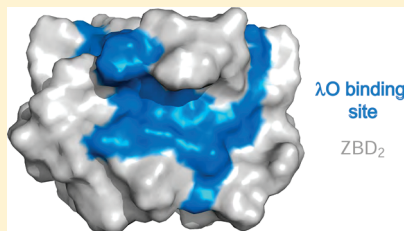


Role of the N-Terminal Domain of the Chaperone ClpX in the Recognition and Degradation of Lambda Phage Protein O

Guillaume Thibault[†] and Walid A. Houry*

Department of Biochemistry, University of Toronto, 1 King's College Circle, Medical Sciences Building, Toronto, Ontario M5S 1A8, Canada

ABSTRACT: The ClpXP ATPase–protease complex is a key element of the protein quality control machinery in the cell. ClpX consists of a zinc-binding domain (ZBD) that forms dimers and a AAA⁺ domain that arranges into a hexamer in an ATP-dependent manner. Here, we report the binding site of the ClpX substrate λ phage protein O (λO) on ZBD₂ in ClpX using NMR and mutagenesis analysis. λO protein was found to interact with a hydrophobic patch on the larger surface of ZBD₂. The affinity of λO toward ZBD₂ was investigated using a quantitative optical biosensor method of dual polarization interferometry. The data suggest overlapping binding sites of λO and the ClpX cofactor SspB on the ZBD₂. Interestingly, a single key mutation in ZBD was found to enhance the ClpXP-dependent degradation of λO.



INTRODUCTION

Protein degradation by ATP-dependent proteases is a critical step in the control of many cellular processes in both prokaryotes and eukaryotes.¹ Cylindrical proteases form large oligomers in which the proteolytic active sites are sequestered within an internal chamber. Access to the chamber is regulated by narrow axial pores that exclude entry of large polypeptides; dysregulation of these proteases by increasing the axial pore size using small molecules is lethal to the cell.^{2–4} Typically, these proteases form complexes with ATPases associated with diverse cellular activities (AAA⁺) superfamily chaperones. The ATPases function to denature and translocate the target substrates to the associated protease proteolytic chamber for degradation.⁵

ClpX and ClpP of *Escherichia coli* form a typical chaperone–cylindrical protease complex.⁶ ClpP is a tetradecameric serine protease consisting of two heptameric doughnut-shaped rings.⁷ ClpX is a AAA⁺ ATPase belonging to the Clp/Hsp100 family. It has a C4-type zinc-binding domain (ZBD) at the N-terminus and a AAA⁺ domain at the C-terminus (Figure 1A).^{8–10} The ZBD forms a very stable constitutive symmetric dimer in isolation and in full-length ClpX. The ZBD dimer interface consists of highly conserved hydrophobic residues.^{8,10} The AAA⁺ domain forms a hexameric doughnut-shaped ring complex in a nucleotide-dependent manner. In that context, the ZBD dimer in the ClpX hexamer might come together to form a trimer-of-dimers during the chaperone functional cycle.^{9,11}

The recognition of some substrates by ClpX is influenced by specific proteins, termed cofactors, which are essential in some cases. Following binding, substrate denaturation by ClpX is the subsequent critical step toward substrate degradation (Figure 1B). Substrate unfolding was proposed to be the rate-limiting step in protein degradation.¹² The unfolded polypeptide is then translocated from ClpX into the ClpP chamber. Within the ClpP proteolytic chamber, polypeptides are degraded into small peptides and, as proposed by our group, are released through

dynamically formed side pores near the ClpP equatorial region^{13–15} (Figure 1B).

ClpX was first isolated based on its ability to degrade the bacteriophage λ replication initiation protein λO.^{16,17} The bacteriophage λO protein is necessary for the initiation of λ DNA replication during the lytic phase life cycle of the phage.¹⁸ λO binds to four direct 19 bp inverted repeat sequences that are part of the oriλ sequence forming the DNA-nucleoprotein structure, O-some.^{19,20} The protein λP and host DnaB, necessary for λ DNA replication, are recruited by the initial formation of the O-some, leading to the formation of the preprimosome. ClpXP was found to mediate the degradation of free λO only, suggesting that O-some formation followed by the preprimosome formation increasingly stabilizes λO against proteolysis. Therefore, ClpXP does not seem to have significant effect on the lysis or lysogeny decision of λ phage because λO is protected when bound to λ DNA.²¹

ClpX also functions as a molecular chaperone toward λO by blocking the thermal inactivation and aggregation of the protein.²² Moreover, ClpX reactivates denatured λO by disaggregating preformed aggregates. λO protein is composed of an N-terminal domain that mediates DNA interactions and a C-terminal domain that is responsible for protein–protein interactions. It was reported that the N-terminal sequence in λO plays the most critical role in facilitating degradation by ClpXP²³ and that two distinct λO structural elements are required for efficient degradation by ClpXP. On the basis of peptide array analysis, our group proposed that residues Gln⁴⁹–Met⁶⁷ of λO preferably bind the N-terminus of ClpX.¹¹

Special Issue: Harold A. Scheraga Festschrift

Received: December 13, 2011

Revised: February 16, 2012

Published: February 23, 2012

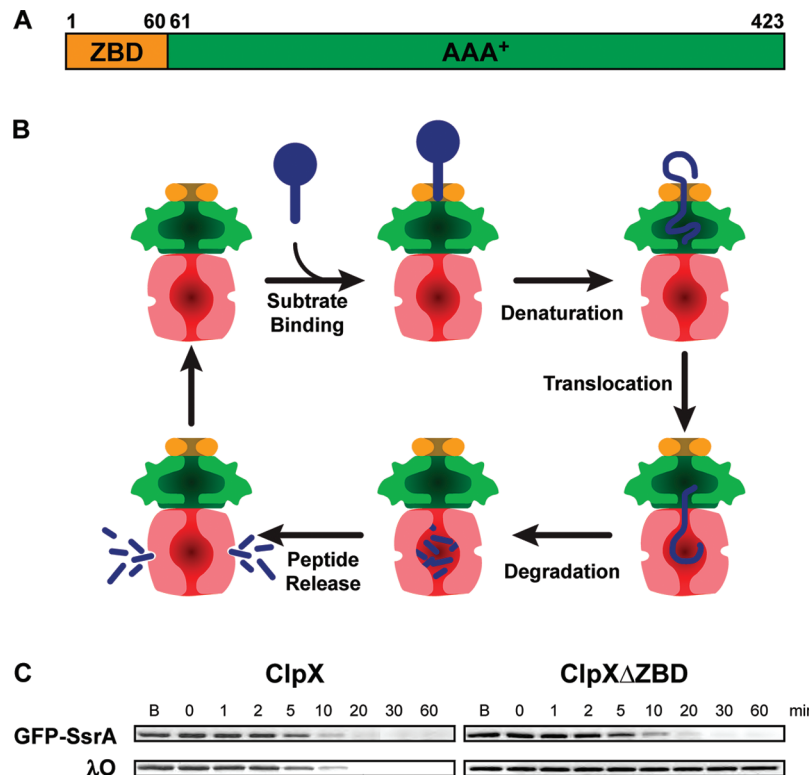


Figure 1. The role of the N-terminus of ClpX in substrate degradation. (A) The domain boundaries of ZBD and AAA⁺ in ClpX. (B) Model of the substrate degradation cycle by ClpXP, where the trimer-of-dimers ZBD, the hexamer AAA⁺ of ClpX, the tetradecamer ClpP, and the substrate are illustrated in orange, green, red, and blue, respectively. Transverse sections are shown to highlight ClpX and ClpP chambers. See the text for a description of the substrate degradation cycle. (C) Degradation of GFP-SsrA and λO by ClpXP or ClpXΔZBDClpP was monitored by SDS-PAGE. The chaperone was the last component added to the reaction mixture. “B” refers to before addition of the chaperone.

In addition to λO, several other exogenous and endogenous substrates were identified for *E. coli* ClpX.^{24–28} Furthermore, ClpXP has been implicated in the degradation of C-terminally SsrA-tagged proteins. GFP with an SsrA sequence (AANDE-NYALAA) added to its C-terminus has been used as a model substrate for biochemical studies.²⁹ The dimeric SspB cofactor enhances the degradation rate of C-terminally SsrA-tagged proteins by ClpXP.³⁰ The substrate binding domain of SspB is located at the N-terminus, while the SspB unstructured C-terminal domain binds to the ZBD of ClpX.³¹ We previously demonstrated that the SspB C-terminus binds to a hydrophobic region on the ZBD₂ surface using NMR approaches,¹¹ and this was independently confirmed later by X-ray crystallography.¹⁰ Here, we characterize and map the binding site of λO on ZBD₂ using NMR spectroscopy, mutational analysis, and thermodynamic interaction studies. We propose that the binding sites of λO and SspB₂ overlap on the ZBD of ClpX. In the course of this work, a ClpX mutant was also identified that enhances the ClpP-dependent degradation of λO relative to wildtype (WT) ClpX.

EXPERIMENTAL METHODS

Protein Purification. All proteins used in this study (ClpX, ClpP, GFP-SsrA, and λO) were expressed and purified as previously described.^{9,32} Point mutations were introduced using the Quick Change system (Stratagene) according to the manufacturer’s protocol. All constructs were verified by DNA sequencing. Protein concentrations were determined using the Bradford assay (Bio-Rad). All reported concentrations are typically those of monomers, unless indicated.

Degradation Assays. Assays were typically carried out by preincubating 1.5 units of creatine kinase, 16 mM creatine phosphate, 3 mM ATP, 4 μM substrate protein, and 1 μM ClpP in buffer A (25 mM HEPES, 5 mM MgCl₂, 5 mM KCl, 0.03% Tween-20, and 10% glycerol) at 37 °C for 3 min. Subsequently, 1 μM ClpX or ClpX mutant was added to the reaction, and the incubation was continued at 37 °C. All concentrations were those of monomers. Samples were taken at the indicated time points, and the degradation was stopped by addition of 4× Laemmli buffer and boiling. Proteins were then separated on SDS-PAGE gels, and the intensities of the protein bands (IPB) were quantified using ImageQuant. The initial rate (V_0) was calculated from the slope of the plot of ln(IPB) versus time for the first 5 min of the reaction. Degradation of GFP-SsrA was also monitored by fluorescence using a Fluorolog spectrophotofluorometer (Jobin Yvon) with the excitation wavelength set at 395 nm and the emission wavelength set at 509 nm.

NMR Spectroscopy. Uniformly ¹⁵N-labeled ZBD₂ was prepared by growing the *E. coli* strain BL21-Gold in minimal media containing ¹⁵NH₄Cl. The NMR sample concentration was 0.25 mM ZBD₂ in buffer B (50 mM sodium phosphate, pH 7.6, 150 mM NaCl, and 10% D₂O). NMR spectra were recorded at 20 °C on a 500 MHz Varian spectrometer. ¹H,¹⁵N heteronuclear single quantum correlation (HSQC) experiments were carried out in the absence or presence of 0.25 mM λO protein.

Measuring Binding Affinities. The binding experiment was performed using an AnaLight Bio200 dual waveguide interferometer instrument from Farfield Group Ltd. (Manchester, U.K.).³³ Experiments were performed in buffer C (50 mM

potassium phosphate, pH 8, 75 mM NaCl, and 1 mM DTT) at a flow rate of 0.05 mL/min, and 0.5 mg/mL of ZBD₂ were cross-linked to both channels of the sensor chip by incubating with [bis(sulfosuccinimidyl)suberate] (BS³) (Pierce Biotechnology). Free BS³ was blocked using 10 mg/mL of glucosamine. Following the establishment of a stable buffer baseline, λO was injected into one channel while the second channel was used as a reference.

■ RESULTS

ZBD Modulating the Degradation of the Bacteriophage Protein λO by ClpXP. The degradation of GFP-SsrA and λO was carried out at 37 °C in the presence of ClpP, ATP, ATP regenerating system, and ClpX or ClpX mutant lacking ZBD, denoted as ClpXΔZBD (Figure 1C, top panel). Samples were withdrawn from the degradation assay mixture at different time points, boiled in Laemmli buffer to stop the reaction, and separated on SDS-PAGE gels. The ClpP-dependent degradation of GFP-SsrA occurred at a similar rate in the presence of WT ClpX and ClpXΔZBD, consistent with previous observations that the primary binding site for the SsrA tag is in the AAA⁺ domain of ClpX and does not require the ZBD.^{9,11} On the other hand, ZBD is essential for the binding and/or denaturation of λO because no λO degradation could be detected in the presence of ClpXΔZBDClpP (Figure 1C, bottom panel).⁹ Thus, ZBD plays an essential role in the binding and/or unfolding of λO by ClpX.

λO and SspB Binding Sites on the Surface of ZBD₂ Overlap but Are Not Identical. Most residues of the N-terminus of ClpX are highly conserved among 103 bacteria, especially between the residues 15 and 48 (Figure 2A). The residues Phe¹⁶, Ile²⁸, Val³³, Ile³⁵, Val⁴⁰, Cys⁴³, and Ile⁴⁷ that form the core of the ZBD dimer interface are generally highly conserved.⁸ ZBD₂ forms a box-shaped structure with four main surfaces. The highly charged surface of ZBD₂ is shown in Figure 2B (top view, column 2); two identical large hydrophobic surfaces are present on both sides of the ZBD₂ box (side view, column 2), and a fourth small hydrophobic surface exists on the opposite side of the highly charged surface (not shown).

To characterize the λO binding site on ZBD, ¹H, ¹⁵N HSQC spectra were recorded for a uniformly ¹⁵N-labeled ZBD₂ in the presence of equal concentrations of λO (Figure 2C). Obtaining a spectrum at higher λO concentration was not possible due to limited protein stability. The chemical shifts of several ZBD residues (Phe¹⁶, Lys²⁶, Leu²⁷, Ile²⁸, Ala²⁹, Tyr³⁴, Asp³⁷, Cys³⁹, Asp⁴¹, Leu⁴², and Cys⁴³) disappeared upon addition of λO (Figure 2C). Residues Phe¹⁶, Leu²⁷, Ile²⁸, Ala²⁹, Tyr³⁴, Cys³⁹, Leu⁴², and Cys⁴³ are part of the ZBD₂ hydrophobic side surfaces (Figure 2B,D). The charged residues Lys²⁶, Asp³⁷, and Asp⁴¹ might also contribute to the binding of λO to ZBD. We previously found the binding site of SspB₂ to be located on the large hydrophobic surfaces of ZBD₂, which is in agreement with the crystal structure of the complex between SspB-tail and ZBD₂.^{10,11} The binding pocket of SspB-tail includes the residues Phe¹⁶, Cys¹⁷, Gln²¹, Lys²⁶, Leu²⁷, Ala²⁹, Gly³⁰, Tyr³⁴, and Ile⁴⁶ (Figure 2B, column 3). In the same study, we also showed that the degradation of λO by ClpXP is severely slowed down in the presence of SspB-tail peptide, suggesting an overlap of the λO and the SspB binding sites on ClpX¹¹. Therefore, these results suggest that λO and SspB binding sites are on the ZBD₂ hydrophobic side surfaces.

Subsequently, mutagenesis analysis of the ZBD in ClpX was carried out. The degradation of λO and GFP-SsrA was

performed at 37 °C in the presence of ClpP and different ClpX mutants. The initial degradation rate of λO was slower in the presence of the ClpX mutants F16W, K26D, D37N/E38Q, E38Q/D41N/D45N, and I46K when compared to that for WT ClpX (Table 1). There was no λO degradation observed for ClpX(L27S) because its ZBD is unstructured.³² In contrast, λO degradation was not affected by ClpX(L27M), suggesting that its ZBD is properly folded. Interestingly, λO degradation was accelerated in the presence of ClpX(Y34W) compared to that for WT (Table 1 and Figure 3). All of the point mutations of ZBD residues in ClpX, with the exception of A29N, also slowed GFP-SsrA degradation compared to that of WT. Although the mechanistic basis for this effect of the mutations was not further investigated here, we speculate that the mutations might indirectly reduce the binding (or recognition) of the SsrA tag to the AAA⁺ domain of ClpX. The mutation of other residues in ZBD that were identified by NMR as possible binding sites for λO generally resulted in misfolded ZBD or ClpX.

The results from the mutational analysis (Table 1) generally correlate with those from the NMR titration experiments, especially for ZBD residues whose chemical shifts disappeared upon addition of λO (Figure 2C,D), namely, Phe¹⁶, Lys²⁶, Tyr³⁴, Asp³⁷, and Asp⁴¹. However, while the NH chemical shift for Leu²⁷ and Ala²⁹ disappeared upon addition of λO, the degradation of λO was not affected by making conservative mutation to these residues.

To further characterize the binding site of λO on ZBD using the generated ClpX mutants, we performed a competition assay. The degradation of 4 μM GFP-SsrA was monitored by fluorescence at 37 °C in the presence of ClpP, ClpX mutants, and various concentrations of λO (Figure 4A,B). Interestingly, the presence of 2 or 4 μM λO was sufficient to slow down the degradation by WT ClpXP of 4 μM GFP-SsrA (Figure 4B). In all cases, λO degradation proceeded faster (before) than GFP-SsrA degradation (Figure 4C), although the rates of degradation of λO alone or GFP-SsrA alone by WT ClpXP are similar (Figure 1C and Table 1). The presence of 10 μM λO was sufficient to significantly inhibit the degradation of 4 μM GFP-SsrA by ClpXP (Figure 4A,B). These results strongly suggest that WT ClpX has a higher affinity for λO than GFP-SsrA. As expected, λO did not affect the ClpP-mediated degradation of GFP-SsrA in the presence of ClpXΔZBD (Figure 4A,B) or ClpX(L27S) (Figure 4A) mutants because neither mutant binds λO. A reduced inhibitory effect of λO on the ClpP-dependent degradation of GFP-SsrA by ClpX mutant would indicate a reduction in the binding affinity of λO to the mutated ClpX. ClpX(F16W), ClpX(L27M), ClpX(A29N), and ClpX(I46K) follow this reasoning (Figure 4A), suggesting the importance of the residues Phe¹⁶, Leu²⁷, Ala²⁹, and Ile⁴⁶ for λO binding.

Interestingly, 4 μM λO resulted in almost complete inhibition of GFP-SsrA degradation mediated by ClpX(Y34W), unlike that for WT ClpX, which required higher concentrations of λO to significantly inhibit GFP-SsrA degradation (Figure 4B). This suggests that the introduction of Trp at position 34 significantly increases the ClpX binding affinity for λO. On the other hand, no significant changes in GFP-SsrA degradation in the presence of 10 μM λO were observed for ClpX(R25Q/K26Q), ClpX(K26D), ClpX(D37N/E38Q), and ClpX(E38Q/D41N/D45N) when compared to WT ClpX, indicating that the charged surface of ZBD₂ is not involved in λO binding.

Measuring the Binding Affinity of the Interaction of λO and ZBD₂. To further characterize the binding of λO to ZBD₂, binding experiments were performed using an *AnaLight*

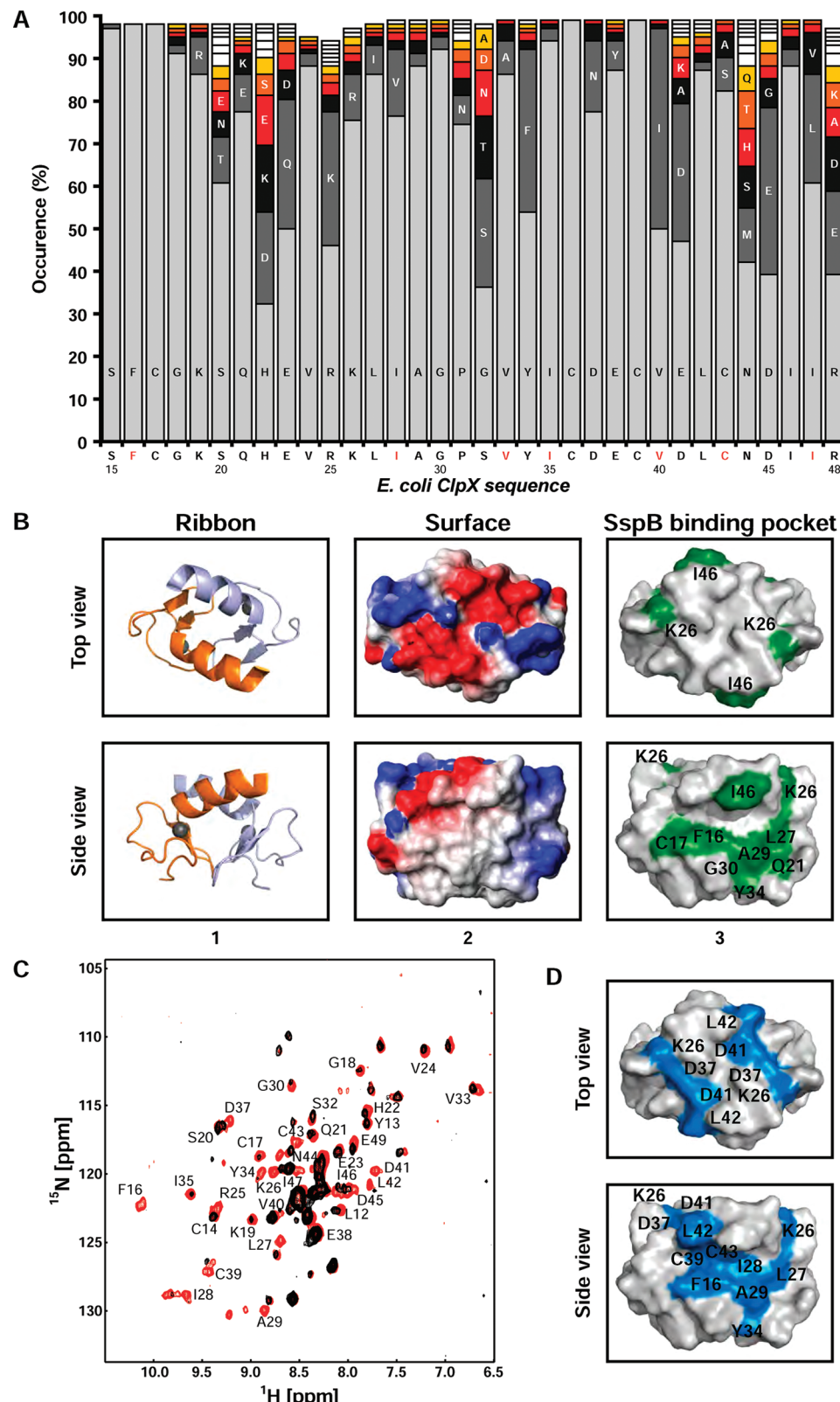


Figure 2. Sequence conservation and structure of ZBD. (A) ClpX sequences from 103 different bacteria were aligned using ClustalW.⁴¹ Residue numbering is according to UniProt *E. coli* ClpX protein. Conserved hydrophobic residues of the ZBD dimer interface are in red font. Bars less than 100% are due to the absence of residues at the corresponding positions in some bacteria. (B) Ribbon and surface representation of ZBD dimer (Protein Data Bank 1OVX). The bottom panel is rotated 90° along the horizontal axis with respect to top panel. In column 1, each subunit of ZBD₂ is represented in orange and light blue, while the Zn(II) atoms are shown as gray spheres. In column 2, the electrostatic surface potential of ZBD₂ is shown with negatively charged, positively charged, and hydrophobic residues in red, blue, and gray, respectively. In column 3, the proposed binding site of the cofactor SspB₂ on the surface of ZBD₂ is shown in green.¹¹ (C) An HSQC spectrum of 0.25 mM ^{15}N -labeled ZBD₂ in the absence (red) or the presence of 0.25 mM λO (black). (D) Residues for which chemical shifts disappeared in the presence of λO are highlighted in blue. All structures were drawn using PyMOL (www.pymol.org).

Table 1. Initial Rates of ClpP-Dependent Degradation of λO and GFP-SsrA Mediated by Different ClpX Mutants^a

	V_0 (10^{-3} s $^{-1}$)	
	λO	GFP-SsrA
ClpX WT	2.1 (0.3)	2.7 (0.4)
ClpX Δ ZBD	no degradation	1.7 (0.1)
F16W	1.0 (0.2)	1.1 (0.1)
R25Q/K26Q	2.0 (0.2)	1.0 (0.4)
K26D	1.6 (0.6)	1.3 (0.3)
L27M	2.0 (0.5)	1.2 (0.3)
L27S	no degradation	1.3 (0.1)
A29N	2.2 (0.5)	2.6 (0.5)
Y34W	6.8 (0.6)	2.1 (0.2)
D37N/E38Q	1.4 (0.2)	1.5 (0.2)
E38Q/D41N/D45N	0.8 (0.1)	2.0 (0.2)
I46K	1.3 (0.1)	1.9 (0.6)

^aInitial rates (V_0) were calculated as described in the Experimental Methods section. The numbers in brackets refer to the standard deviation from three repeats.

Bio200 dual waveguide interferometer instrument from Farfield Group Ltd. (Manchester, U.K.).^{11,33,34} ZBD₂ was cross-linked to the sensor chip by using bis(sulfosuccinimidyl)suberate

(BS³). After the establishment of a stable buffer baseline, λO protein was injected over the immobilized ZBD₂. The thickness and density of λO interacting with ZBD₂ on the sensor chip were measured. Therefore, the mass change on the surface of the sensor chip as a function of injected sample concentration could be followed (Figure 5A). Mass change data were fit to a model of two independent binding events, giving a very good fit to the experimental points (Figure 5B). This result suggests that one molecule of λO binds on each side of ZBD₂ because the stoichiometry $\lambda O/ZBD_2$ was 2:1. The weak association reaction of λO to ZBD₂ had a K_d of 59.6 μM , while the strong association reaction had a K_d of 0.59 μM (Table 2). This suggests that the binding of one λO to ZBD₂ dramatically increases the binding affinity for a second λO .

DISCUSSION

We have demonstrated that the binding site of λO is located on the N-terminus of ClpX. NMR spectroscopy, degradation assays, and competition assays suggest that the binding site of λO is located on the hydrophobic surface of ZBD₂. The NMR data of Figure 2C,D implicated the following residues in binding to λO : Phe¹⁶, Lys²⁶, Leu²⁷, Ile²⁸, Ala²⁹, Tyr³⁴, Asp³⁷, Cys³⁹, Asp⁴¹, Leu⁴², and Cys⁴³; the mutational analysis of Table 1

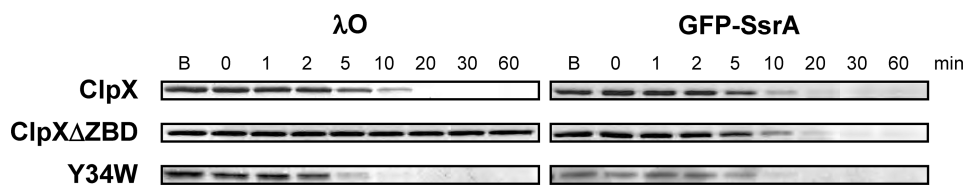


Figure 3. ClpP-dependent degradation of λO in the presence of different ClpX mutants. Degradation assays were carried out at 37 °C by preincubating ClpP, λO or GFP-SsrA, ATP, and ATP regenerating system and then adding ClpX or ClpX mutant. Aliquots were removed at different time points and then visualized on SDS-PAGE gels. Initial rates (V_0) for the degradation of λO and GFP-SsrA are given in Table 1.

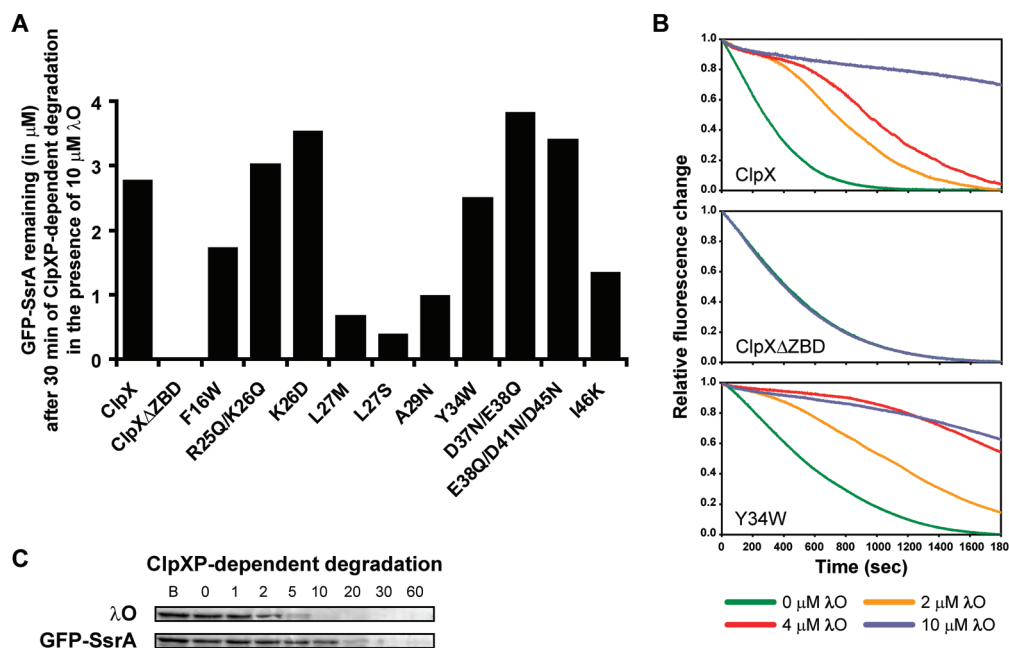


Figure 4. The effect of λO on GFP-SsrA degradation by ClpX mutants and ClpP. (A) The concentration of GFP-SsrA remaining after 30 min of ClpP-dependent degradation mediated by ClpX/ClpX mutants in the presence of 10 μM of λO . The initial concentration of GFP-SsrA was 4 μM . (B) The ClpP-dependent degradation of GFP-SsrA mediated by ClpX, ClpX Δ ZBD, or ClpX(Y34W) and ClpP was carried out in the presence of increasing concentration of λO and monitored by fluorescence. (C) Degradation of a mixture of 4 μM GFP-SsrA and 4 μM λO by WT ClpXP. Aliquots were removed at different times points and then visualized on SDS-PAGE gels.

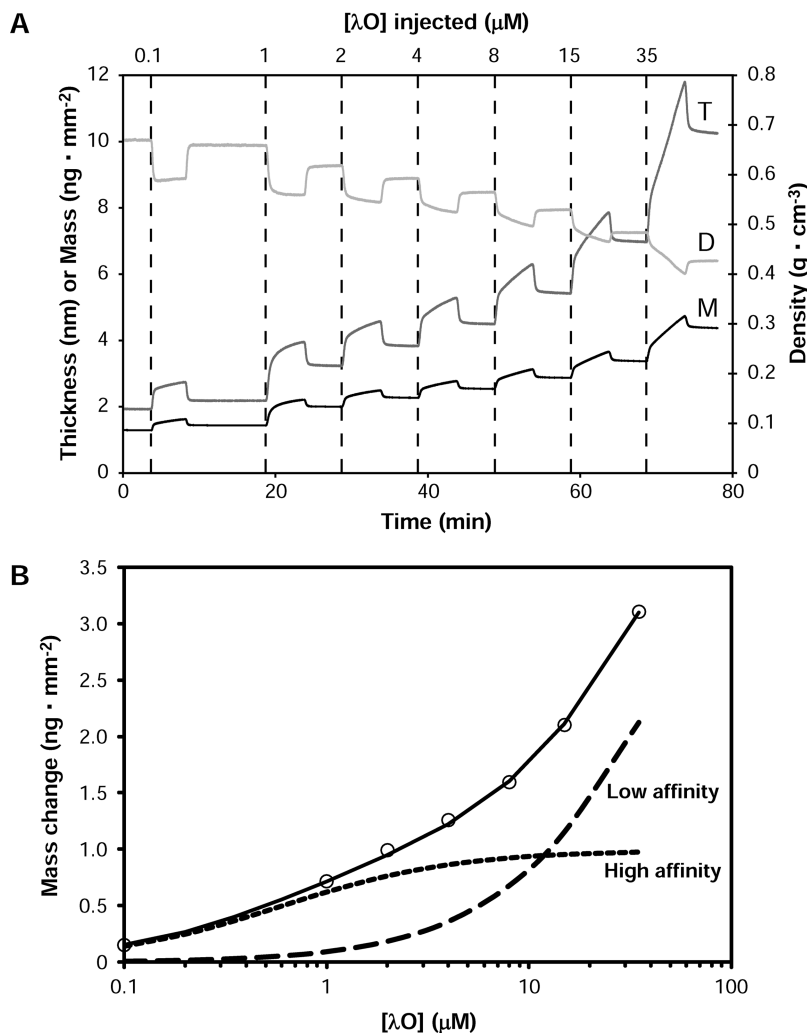


Figure 5. Determination of the binding affinity of λO to ZBD_2 using dual polarization interferometry. (A) Raw sensor data upon addition of free λO to immobilized ZBD_2 . T, D, and M refer to thickness, density, and mass, respectively. Different additions of λO are indicated with dashed lines. The concentrations of injected λO are shown on the top x-axis. (B) Open circles represent the experimental binding data of λO to ZBD_2 , whereas the solid line represents the theoretical fit to the data assuming two independent binding events. Curves drawn with short- and long-dashed lines represent the theoretical binding curves, assuming a single binding event with K_d values given in Table 2 corresponding to the high- and low-affinity interactions.

Table 2. Binding Parameters of λO and $SspB$ to ZBD_2 Obtained from the Fits to the Experimental Data of Figure 5

	λO		$SspB_2^b$	
	high affinity	low affinity	high affinity	low affinity
K_d (μM) ^a	0.59	59.60	0.85	11.00
k_a ($s^{-1} M^{-1}$) ^a	8000	150	1940	540
k_d (s^{-1}) ^a	0.005	0.009	0.002	0.006

^aThe standard deviations on the numbers are estimated to be about 10% of the respective values. ^bPreviously published values for the binding of $SspB_2$ to ZBD_2 are given in ref 11.

and Figure 3 implicated the following residues: Phe¹⁶, Lys²⁶, Tyr³⁴, Asp³⁷, Glu³⁸, Asp⁴¹, Asp⁴⁵, and Ile⁴⁶; and the competition assays of Figure 4 implicated the following residues: Phe¹⁶, Leu²⁷, Ala²⁹, Tyr³⁴, and Ile⁴⁶. Hence, Phe¹⁶ and Tyr³⁴ seem to be the most critical residues for λO binding on the hydrophobic patch of ZBD of ClpX as they have been implicated in such binding by all three approaches used.

Other substrates, cofactors, and adaptors have been shown to also bind the N-terminus of ClpX.^{9,35–39} This suggests that the hydrophobic patch on the surface of ZBD_2 is the major binding site for substrates and cofactors that are ZBD-dependent for degradation by ClpXP. Interestingly, the amino acid sequence of the N-terminus of λO is similar to that of the N-terminus of the stationary-phase sigma factor σ^S and the starvation stress DNA binding protein Dps, which is also degraded by ClpX²⁸. Hence, we speculate that the N-terminus of σ^S and Dps bind to the same site on ZBD as that of λO . On the other hand, MuA phage protein, the transcriptional regulator YbaQ, and the riboflavin biosynthesis enzyme RibB, which are also degraded by ClpXP²⁸, have similar C-terminal motifs, R⁶⁵⁸RKKAI⁶⁶³, R¹⁰⁸AKKVA¹¹³, and H²¹²ERKAS²¹⁷, respectively, which are relatively similar to the $SspB$ C-terminus R¹⁶²VVK¹⁶⁵. Thus, MuA, YbaQ, and RibB possibly bind to the same $SspB$ binding site on ZBD. Hence, it is apparent that many *E. coli* proteins are recognized by the N-terminus of ClpX for degradation. This large spectrum of proteins is expected to compete for ZBD binding, and this competition leading to protein degradation

might regulate several biological functions. In this context, ClpXP is expected to degrade proteins according to their respective binding affinity to the N-terminus of ClpX and their relative abundance in bacteria.

Under certain stress conditions, cofactors favor the degradation of specific substrates by increasing their binding affinity to ClpXP. For instance, ClpXP binding affinity for SsrA-tagged proteins is around $1 \mu\text{M}$, which is similar to the λO binding affinity (Table 2 and ref 40). To increase the degradation rate of SsrA-tagged proteins during stress conditions, formation of a SspB/SsrA-tagged-protein/ClpXP complex significantly increases the apparent binding affinity of SspB-SsrA for ClpX to $0.2 \mu\text{M}$,⁴⁰ resulting in fast degradation of SsrA-tagged proteins over other ClpXP substrates. The zinc-binding domain of ClpX clearly plays a critical role in the control of many cellular processes by selecting substrates to be degraded by the ClpXP complex.

CONCLUSION

Here, we have elucidated the binding site for λO on the ZBD of ClpX. The identified site is found to overlap with that for the binding of SspB to ClpX and is on the hydrophobic faces of ZBD₂. Therefore, the ClpX hexamer potentially contains six binding sites for λO , where two are found for each ZBD₂. Interestingly, the mutation of Y34W in the ZBD of ClpX was found to enhance the ClpXP-dependent degradation of λO . The identification of such a mutant might suggest that yet to be identified cofactors or other chaperones could function with ClpX to enhance the ClpP-dependent degradation of λO .

AUTHOR INFORMATION

Corresponding Author

*Tel.: +416 946 7141. Fax: +416 978 8548. E-mail: walid.houry@utoronto.ca.

Present Address

[†]Temasek Life Sciences Laboratory, 1 Research Link, National University of Singapore, 117604, Singapore.

Notes

The authors declare no competing financial interest.

ACKNOWLEDGMENTS

We thank Dr. Remco Sprangers for help with the NMR experiments. G.T. held graduate fellowships from the Natural Sciences and Engineering Research Council of Canada and also received a graduate fellowship from the Fonds Québécois de la Recherche sur la Nature et les Technologies. This work was supported by a grant to W.A.H. from the Canadian Institutes of Health Research (MOP-67210).

ABBREVIATIONS USED

AAA⁺, ATPases Associated with diverse cellular Activities; GFP-SsrA, green fluorescent protein with a C-terminal SsrA tag (AANDENYALAA); ZBD, zinc-binding domain

REFERENCES

- (1) Wickner, S.; Maurizi, M. R.; Gottesman, S. *Science* **1999**, 286, 1888–1893.
- (2) Thompson, M. W.; Maurizi, M. R. *J. Biol. Chem.* **1994**, 269, 18201–18208.
- (3) Brotz-Oesterhelt, H.; Beyer, D.; Kroll, H. P.; Endermann, R.; Ladel, C.; Schroeder, W.; Hinzen, B.; Raddatz, S.; Paulsen, H.; Henninger, K.; et al. *Nat. Med.* **2005**, 11, 1082–1087.
- (4) Leung, E.; Datti, A.; Cossette, M.; Goodreid, J.; McCaw, S. E.; Mah, M.; Nakhamchik, A.; Ogata, K.; El Bakkouri, M.; Cheng, Y. Q.; et al. *Chem. Biol.* **2011**, 18, 1167–1178.
- (5) Baker, T. A.; Sauer, R. T. *Biochim. Biophys. Acta* **2012**, 1823, 15–28.
- (6) Schirmer, E. C.; Glover, J. R.; Singer, M. A.; Lindquist, S. *Trends Biochem. Sci.* **1996**, 21, 289–296.
- (7) Wang, J.; Hartling, J. A.; Flanagan, J. M. *Cell* **1997**, 91, 447–456.
- (8) Donaldson, L. W.; Wojtyra, U.; Houry, W. A. *J. Biol. Chem.* **2003**, 278, 48991–48996.
- (9) Wojtyra, U. A.; Thibault, G.; Tuite, A.; Houry, W. A. *J. Biol. Chem.* **2003**, 278, 48981–48990.
- (10) Park, E. Y.; Lee, B. G.; Hong, S. B.; Kim, H. W.; Jeon, H.; Song, H. K. *J. Mol. Biol.* **2007**, 367, 514–526.
- (11) Thibault, G.; Yudin, J.; Wong, P.; Tsitrin, V.; Sprangers, R.; Zhao, R.; Houry, W. A. *Proc. Natl. Acad. Sci. U.S.A.* **2006**, 103, 17724–17729.
- (12) Kim, Y. I.; Burton, R. E.; Burton, B. M.; Sauer, R. T.; Baker, T. A. *Mol. Cell* **2000**, 5, 639–648.
- (13) Gribun, A.; Kimber, M. S.; Ching, R.; Sprangers, R.; Fiebig, K. M.; Houry, W. A. *J. Biol. Chem.* **2005**, 280, 16185–16196.
- (14) Sprangers, R.; Gribun, A.; Hwang, P. M.; Houry, W. A.; Kay, L. E. *Proc. Natl. Acad. Sci. U.S.A.* **2005**, 102, 16678–16683.
- (15) Kimber, M. S.; Yu, A. Y.; Borg, M.; Leung, E.; Chan, H. S.; Houry, W. A. *Structure* **2010**, 18, 798–808.
- (16) Gottesman, S.; Clark, W. P.; de Crecy-Lagard, V.; Maurizi, M. R. *J. Biol. Chem.* **1993**, 268, 22618–22626.
- (17) Wojtkowiak, D.; Georgopoulos, C.; Zylicz, M. *J. Biol. Chem.* **1993**, 268, 22609–22617.
- (18) Roberts, J. D.; McMacken, R. *Nucleic Acids Res.* **1983**, 11, 7435–7452.
- (19) Dodson, M.; Roberts, J.; McMacken, R.; Echols, H. *Proc. Natl. Acad. Sci. U.S.A.* **1985**, 82, 4678–4682.
- (20) Schnos, M.; Zahn, K.; Inman, R. B.; Blattner, F. R. *Cell* **1988**, 52, 385–395.
- (21) Zylicz, M.; Liberek, K.; Wawrzynow, A.; Georgopoulos, C. *Proc. Natl. Acad. Sci. U.S.A.* **1998**, 95, 15259–15263.
- (22) Wawrzynow, A.; Wojtkowiak, D.; Marszalek, J.; Banecki, B.; Jonsen, M.; Graves, B.; Georgopoulos, C.; Zylicz, M. *EMBO J.* **1995**, 14, 1867–1877.
- (23) Gonciarz-Swiatek, M.; Wawrzynow, A.; Um, S. J.; Learn, B. A.; McMacken, R.; Kelley, W. L.; Georgopoulos, C.; Sliekers, O.; Zylicz, M. *J. Biol. Chem.* **1999**, 274, 13999–14005.
- (24) Lehnher, H.; Yarmolinsky, M. B. *Proc. Natl. Acad. Sci. U.S.A.* **1995**, 92, 3274–3277.
- (25) Frank, E. G.; Ennis, D. G.; Gonzalez, M.; Levine, A. S.; Woodgate, R. *Proc. Natl. Acad. Sci. U.S.A.* **1996**, 93, 10291–10296.
- (26) Levchenko, I.; Yamauchi, M.; Baker, T. A. *Genes Dev.* **1997**, 11, 1561–1572.
- (27) Zhou, Y.; Gottesman, S. *J. Bacteriol.* **1998**, 180, 1154–1158.
- (28) Flynn, J. M.; Neher, S. B.; Kim, Y. I.; Sauer, R. T.; Baker, T. A. *Mol. Cell* **2003**, 11, 671–683.
- (29) Weber-Ban, E. U.; Reid, B. G.; Miranker, A. D.; Horwich, A. L. *Nature* **1999**, 401, 90–93.
- (30) Levchenko, I.; Seidel, M.; Sauer, R. T.; Baker, T. A. *Science* **2000**, 289, 2354–2356.
- (31) Dougan, D. A.; Weber-Ban, E.; Bukau, B. *Mol. Cell* **2003**, 12, 373–380.
- (32) Thibault, G.; Tsitrin, Y.; Davidson, T.; Gribun, A.; Houry, W. A. *EMBO J.* **2006**, 25, 3367–3376.
- (33) Cross, G. H.; Reeves, A. A.; Brand, S.; Popplewell, J. F.; Peel, L. L.; Swann, M. J.; Freeman, N. J. *Biosens. Bioelectron.* **2003**, 19, 383–390.
- (34) Swann, M. J.; Peel, L. L.; Carrington, S.; Freeman, N. J. *Anal. Biochem.* **2004**, 329, 190–198.
- (35) Tanaka, N.; Tani, Y.; Hattori, H.; Tada, T.; Kunugi, S. *Protein Sci.* **2004**, 13, 3214–3221.
- (36) Hinnerwisch, J.; Reid, B. G.; Fenton, W. A.; Horwich, A. L. *J. Biol. Chem.* **2005**, 280, 40838–40844.

- (37) Barnett, M. E.; Nagy, M.; Kedzierska, S.; Zolkiewski, M. *J. Biol. Chem.* **2005**, *280*, 34940–34945.
- (38) Chowdhury, T.; Chien, P.; Ebrahim, S.; Sauer, R. T.; Baker, T. A. *Protein Sci.* **2010**, *19*, 242–254.
- (39) Wang, F.; Mei, Z.; Qi, Y.; Yan, C.; Hu, Q.; Wang, J.; Shi, Y. *Nature* **2011**, *471*, 331–335.
- (40) Bolon, D. N.; Wah, D. A.; Hersch, G. L.; Baker, T. A.; Sauer, R. T. *Mol. Cell* **2004**, *13*, 443–449.
- (41) Larkin, M. A.; Blackshields, G.; Brown, N. P.; Chenna, R.; McGgettigan, P. A.; McWilliam, H.; Valentin, F.; Wallace, I. M.; Wilm, A.; Lopez, R.; et al. *Bioinformatics* **2007**, *23*, 2947–2948.